Scientific Journal of Astana IT University
ISSN (P): 2707-9031 ISSN (E): 2707-904X
VOLUME 25, MARCH 2026

DOI: **10.37943/25KZEM7835**

Aigul Kulakayeva
PhD, Associate Professor of the Radio Engineering,
Electronics and Telecommunications Department
a.kulakayeva@iitu.edu.kz, orcid.org/0000-0002-0143-085X
International Information Technology University, Kazakhstan
Berik Zhumazhanov
PhD student, Department of Space Engineering and Technologies
b.zhumazhanov@ghalam.kz, orcid.org/0000-0001-5926-9619
L.N. Gumilyov Eurasian National University, Kazakhstan
Head of the Payload and R&D Department
Ghalam LLP, Kazakhstan
Yevgeniya Daineko
PhD, Associate Professor, Director of the Institute
of Automation and Information Technologies
y.daineko@iitu.edu.kz, orcid.org/0000-0001-6581-2622
Satbayev University, Kazakhstan
PhD, Professor, Department of Computer Engineering
International Information Technology University, Kazakhstan
Aigul Nurlankyzy
PhD, Assistant Professor of the Department of Cyber Security
a.nurlankyzy@iitu.edu.kz, orcid.org/0000-0002-0791-8573
International Information Technology University, Kazakhstan

ASSESSMENT OF PASSIVE DEORBITING OF THE KAZAKH EARTH REMOTE SENSING SATELLITES KAZEOSAT-1 AND KAZEOSAT-2

Abstract: In this work, passive deorbiting of the Kazakh Earth remote sensing satellites KazEOSat-1 and KazEOSat-2, operating in sun-synchronous low Earth orbits and not equipped with onboard deorbiting systems, is investigated. The object of the study is the dynamics of their orbital motion and the processes of aerodynamic drag during the final stage of operation. Using numerical modeling, time-dependent variations of the main orbital elements were obtained, the rates of orbital altitude decay were estimated, and possible timelines for passive deorbiting were evaluated. In addition, a sensitivity analysis of the results to variations in aerodynamic parameters was performed. It was established that the differences in the orbital evolution of the KazEOSat-1 and KazEOSat-2 spacecraft are mainly determined by the combination of orbital altitude and ballistic coefficient. In particular, the lower orbital altitude and smaller ballistic coefficient of KazEOSat-2 lead to more intense aerodynamic drag and, consequently, to accelerated orbital decay. The orbital degradation of KazEOSat-1 occurs at a significantly slower rate. A distinctive feature of the presented results is their applicability to real operating spacecraft that are not equipped with deorbiting systems, as well as the consideration of uncertainties in aerodynamic characteristics, which made it possible to obtain well-grounded estimates of passive deorbiting timelines. The results of the study can be used in planning the end-of-life phase of Earth remote sensing spacecraft, in assessing the risks of non-compliance with international recommendations on orbital deorbiting timelines, and in substantiating the need for passive or active deorbiting systems in the development of future spacecraft of a similar type.

Keywords: deorbiting; spacecraft; Earth remote sensing; KazEOSat-1; KazEOSat-2; satellite; orbit.

Introduction

Earth remote sensing (ERS) satellites typically operate in sun-synchronous low Earth orbits. Such orbits are optimal for optical imaging; however, from the perspective of mission end-of-life, they pose certain

Received: 14.01.2026 Accepted: 25.02.2026 Published: 30.03.2026

DOI: 10.37943/25KZEM7835

challenges. Natural orbital decay at altitudes of 600–800 km occurs extremely slowly. If a spacecraft is not equipped with active deorbiting systems, it may remain in orbit for decades after the end of its operational lifetime.

For the currently operating Kazakh ERS spacecraft KazEOSat-1 and KazEOSat-2, the issue of deorbiting is becoming increasingly relevant. Both spacecraft were launched in 2014 and were not originally designed with the capability for active orbital deorbiting. At the same time, these spacecrafts differ significantly in mass, orbital altitude, and ballistic characteristics, which directly affect the rate of their natural orbital decay.

At present, estimating the timelines of passive deorbiting is challenging. This is due to uncertainties in aerodynamic parameters and the variability of the upper atmospheric density, which in turn depend on solar and geomagnetic activity. In this regard, engineering models and scenario-based analysis are commonly used for forecasting purposes.

In this work, an analysis of the long-term orbital evolution of the KazEOSat-1 and KazEOSat-2 spacecraft is carried out in order to assess the prospects for their passive deorbiting by means of aerodynamic drag. The main focus is placed on comparing the dynamics of orbital parameters and identifying the key factors that determine the rate of orbital decay.

Thus, Zhumazhanov et al. proposed a deorbiting strategy for the KazEOSat-1 satellite [1]. Their study showed that a combination of active braking and subsequent aerodynamic descent provides controlled orbital decay. However, uncertainties related to atmospheric density and the ballistic characteristics of the spacecraft remain.

Similar issues are also noted by Mahapatra, who demonstrated that the rate of orbital descent depends on mass, cross-sectional area, and solar activity [2]. However, without accounting for the specifics of sun-synchronous orbits, the accuracy of the predictions is limited.

Rosengren et al. showed that orbital evolution is significantly influenced by gravitational and resonant effects [3]. However, their modeling requires substantial computational resources.

Alternative mechanisms for accelerating orbital decay are investigated by Smith et al., who showed that ionospheric and electrodynamic drag can increase deorbiting efficiency, but require complex technical solutions [4]. Passive methods, such as aerodynamic sails [5] and area augmentation systems [6], have demonstrated their potential, although their implementation is only possible at the spacecraft design stage. The quality of modeling strongly depends on the accuracy of atmospheric models. The SWAMI project [7] and the work of Vielberg et al. [8] showed that the use of refined atmospheric density models significantly improves the accuracy of predictions.

Practical aspects of accelerated deorbiting of nanosatellites are described by Niccolai and Mengali [9], Walsh et al. [10], and Alshamy et al. [11], who showed that increasing the aerodynamic cross-sectional area and optimizing the spacecraft body shape effectively reduce orbital lifetime.

An analysis of existing studies demonstrates that, despite significant progress in orbital evolution modeling and deorbiting technologies, quantitative estimation of passive deorbiting timelines for specific spacecraft in sun-synchronous orbits remains a challenging task. This issue is particularly relevant for spacecraft without active control and deorbiting systems, whose ballistic and orbital parameters differ substantially.

This article presents a comparative analysis of passive deorbiting of two operational Earth remote sensing spacecraft (KazEOSat-1 and KazEOSat-2). Although both spacecraft belong to the same mission class and operate in sun-synchronous orbits, they differ significantly in mass, orbital altitude, and ballistic coefficient. This makes them a representative case for studying the influence of these parameters on long-term orbital evolution and deorbiting timeline prediction. The work presents numerical modeling of orbital dynamics and a sensitivity analysis of the results with respect to variations in aerodynamic characteristics.

Unlike previous studies that focus on individual spacecraft (e.g., KazEOSat-1 in [1]) or provide generalized dependencies of orbital decay on altitude and ballistic parameters, this work offers a detailed comparative quantification of passive deorbiting dynamics for two operational spacecraft with significantly different characteristics. In addition, the study explicitly incorporates uncertainty ranges of aerodynamic parameters under real operational conditions, allowing for a more robust estimation of deorbiting timelines.

Scientific Journal of Astana IT University
ISSN (P): 2707-9031 ISSN (E): 2707-904X
VOLUME 25, MARCH 2026

This combination of comparative analysis and uncertainty-aware modeling constitutes the main contribution of the present work.

The study was conducted using widely accepted models of gravitational and aerodynamic perturbations, data from open orbital catalogs, and published information on the characteristics of the spacecraft under consideration, as well as results from previous studies on orbital motion and deorbiting modeling. This approach makes it possible to consider the problem comprehensively and to formulate conclusions that are relevant for planning the end-of-life phase of Earth remote sensing spacecraft in the absence of active deorbiting systems.

Methods and Materials

The calculations were performed using the BETsMA software package, developed by specialists of Universidad Carlos III of Madrid in cooperation with Persei (Spain). This package was used for numerical integration of the equations of perturbed motion in a geocentric inertial coordinate system. The model accounted for the central gravitational attraction of the Earth, the influence of the second zonal harmonic of the Earth's gravitational field, as well as aerodynamic drag in the upper atmosphere.

Orbital and ballistic parameters of the KazEOSat-1 and KazEOSat-2 spacecraft obtained from open sources were used as input data for the numerical simulations. In particular, published information from the national space systems operator, data from specialized orbital element catalogs, and open technical descriptions of the spacecraft were analyzed. General reference information on the spacecraft is presented in Tables 1 and 2.

Table 1. General information on the KazEOSat-1 spacecraft

Parameter	Value
Name	KazEOSat-1 [12]
Operator	JSC "NC Kazakhstan Gharysh Sapary" [14]
Manufacturer	Airbus Defence and Space (France) [13]
Launch date	30 April 2014 [12]
Launch vehicle	Vega [14]
Launch site	Kourou (French Guiana) [12]
Orbit type	Low Earth sun-synchronous orbit (SSO) [15]
Orbital altitude	758–760 km [15]
Orbital inclination	98,3°[15]
Orbital period	99,9 min [15]
Revisit period	3 days
Status	Mission active

Table 2. General parameters of the KazEOSat-2 spacecraft

Parameter	Value
Name	KazEOSat-2 (Kazakhstan Earth Observation Satellite-2)
Operator	JSC "NC Kazakhstan Gharysh Sapary" [13]
Manufacturer	SSTL (Surrey Satellite Technology Ltd, United Kingdom) [14]
Platform (bus)	SSTL-150 [14]
Launch date	19 June 2014 [14]
Launch vehicle	Dnepr [14]
Launch site	Yasny Cosmodrome, Russia [14]
Orbit	Sun-synchronous orbit (approximately 630 km) [14]
Mass	177 kg [18]
Spacecraft dimensions	700 × 800 × 900 mm [18]

DOI: 10.37943/25KZEM7835

Design operational lifetime	7 years [14]
Average orbital power	55 W [17]

The calculations took into account parameters that directly affect the orbital motion model and aerodynamic drag, including spacecraft mass, mean altitude of the sun-synchronous orbit, effective aerodynamic cross-sectional area, aerodynamic drag coefficient, and ballistic coefficient. The input parameter values used for modeling the KazEOSat-1 and KazEOSat-2 Earth remote sensing spacecraft are presented in Tables 3 and 4, respectively.

Table 3. Input parameters of the KazEOSat-1 spacecraft used for modeling orbital dynamics and deorbiting

№	Parameter	Value (estimate)	Note
1	Spacecraft mass *(m)*, kg	820	Launch mass [13]
2	Effective aerodynamic cross-sectional area *(A)*, m^2	10–15	Estimate based on spacecraft dimensions with allowance for possible attitude
3	Aerodynamic drag coefficient *(Cd)*	2.0–2.4	Typical range for complex-shaped spacecraft in LEO
4	Mean orbital altitude *(h)*, km	758–760	Sun-synchronous orbit, data from orbital catalogs
5	Orbital inclination *(i)*, degrees	98.3	Typical value for an SSO at this altitude
6	Orbital semi-major axis *(a)*, km	7128	-
7	Orbital eccentricity *(e)*	0.001–0.003	Nearly circular orbit; estimate based on TLE
8	Argument of perigee *(ω)*, degrees	0–360	Rapidly varying parameter for SSO; treated as a variable
9	Ballistic coefficient *(B)*, kg/m^2	25–45	Calculated parameter determined from *m, A,* C_d

Table 4. Orbital and operational parameters of the KazEOSat-2 spacecraft

Parameter	Value
Orbital altitude (approximate)	630 km [17]
Orbital inclination	97.8–98° [18]
Orbital period	97 min [18]
Revisit time	2–3 days [18]

Due to the lack of publicly available full operational data for the spacecraft under consideration, including information on their current configuration, attitude modes, and actual aerodynamic characteristics at the final stage of the mission, the effective aerodynamic cross-sectional area and drag coefficient were specified as ranges of values (Tables 3 and 4). This approach makes it possible to account for uncertainties in real operational conditions.

Atmospheric density in the calculations was determined using the empirical NRLMSISE-00 model, taking into account orbital altitude and parameters of solar–geomagnetic activity. The adopted computational framework, focused on the analysis of long-term orbital evolution and passive deorbiting processes, is not intended for high-precision ballistic navigation tasks. The chosen level of model detail is

Scientific Journal of Astana IT University
ISSN (P): 2707-9031 ISSN (E): 2707-904X
VOLUME 25, MARCH 2026

sufficient for estimating the time scales of orbital decay and for a comparative analysis of the KazEOSat-1 and KazEOSat-2 spacecraft.

To verify the model, the calculated decay curve of the semi-major axis (Figure 1) was compared with archived Two-Line Element (TLE) data from open catalog CelesTrak.org as of 1 November 2025. The agreement between the calculated decay rate (0.5 km/year) and the observed one is within an acceptable range for engineering-level modeling that confirms the adequacy of the adopted range of the aerodynamic drag coefficient Cd (2.0–2.4).

Results

In low Earth sun-synchronous orbits, where aerodynamic drag is the dominant perturbation, the orbital decay rate of a spacecraft, in a first approximation, depends on its ballistic coefficient and the conditions of interaction with the upper atmosphere.

A comparison of the parameters of KazEOSat-1 and KazEOSat-2 shows that the higher orbital altitude and significantly larger mass-to-area ratio of KazEOSat-1 result in a slower evolution of its orbital parameters. These differences are consistent with the trends identified in the modeling results.

Comparative analysis of the influence of differences in the characteristics of KazEOSat-1 and KazEOSat-2 on orbital dynamics

A comparative analysis of the KazEOSat-1 and KazEOSat-2 spacecraft, which are part of a unified national Earth remote sensing system, reveals significant differences in their mass-dimensional, ballistic, and orbital characteristics. These differences determine the distinct nature of their orbital evolution and their varying susceptibility to aerodynamic drag. A generalized assessment of the influence of selected parameters on orbital dynamics is presented in Table 5.

Table 5. Influence of the ballistic parameters of KazEOSat-1 and KazEOSat-2 on orbital dynamics

Parameter	KazEOSat-1	KazEOSat-2	Note
Spacecraft mass (*m*)	820 kg	177 kg	A larger mass leads to an increase in the ballistic coefficient and a reduced sensitivity to aerodynamic drag
Effective aerodynamic cross-sectional area (*A*)	10–15 m²	6–10 m ²	With a smaller area, aerodynamic drag decreases; however, this effect is compensated by the lower mass
Aerodynamic drag coefficient (C_d)	2.0–2.4	2.0–2.4	Comparable values are not a determining factor for the observed differences
Ballistic coefficient (B)	25–45 kg/m²	8–17 kg/m ²	Key parameter: the orbital evolution of KazEOSat-1 proceeds more slowly
Typical attitude assumed in calculations	Stabilized / random	Stabilized / random	Affects the range of *A*
Sensitivity to aerodynamic drag	Low	Medium	Determined by the value of *B*
Mean orbital altitude (*h*)	750–760 km	630 km	The higher orbit of KazEOSat-1 is characterized by a significantly lower atmospheric density
Orbit type	Sun-synchronous	Sun-synchronous	The orbit type is the same; differences are determined by altitude
Atmospheric density at orbit (ρ)	Very low	Low	For KazEOSat-2, aerodynamic perturbations are more pronounced

DOI: 10.37943/25KZEM7835

Rate of change of the semi-major axis	Low	Medium	KazEOSat-2 loses orbital energy more rapidly
Sensitivity to solar activity	Low	Medium	At lower altitudes, density variations have a stronger impact on motion
Long-term orbital evolution	Slow	More intensive	Determined by the combination of altitude and *B*
Need to account for variability of *A* and C_d	High	Medium	For KazEOSat-1, uncertainties have a stronger impact on predictions
Predictability of orbital motion	Higher under identical models	Lower	For KazEOSat-2, stochastic factors have a greater influence

KazEOSat-1 has a significantly higher ballistic coefficient due to its larger mass. As a result, its orbit evolves more slowly compared to KazEOSat-2.

In turn, the lower mass and lower orbital altitude of KazEOSat-2 lead to a stronger influence of aerodynamic drag and, as a result, to a more rapid change in its orbital elements. Thus, differences in ballistic and orbital characteristics determine fundamentally different orbital decay dynamics for these two spacecrafts.

A direct graphical comparison of orbital decay profiles is expected to further illustrate these differences and is considered a direction for future work.

Long-term evolution of the main orbital elements of spacecraft in low Earth sun-synchronous orbit. Based on the available technical and ballistic parameters of the KazEOSat-1 and KazEOSat-2 spacecraft, numerical simulations of their orbital dynamics were performed. The simulations were performed in a geocentric inertial coordinate system with perturbations included, following the approaches described by Sánchez-Arriaga et al. [19] and García Ortiz and Sánchez-Arriaga [20]. The equations of motion are written in vector form as the sum of the central gravitational acceleration and perturbing accelerations:

$$\ddot{r} = a_0 + \sum a_{pert}, \qquad (1)$$

where $\ddot{r}$ – is the spacecraft radius vector, a_0 – the acceleration of the Earth's central gravitational attraction, a_{pert} – the combined perturbing accelerations.

The central gravitational acceleration is described by the following expression:

$$a_0 = -\mu \frac{r}{r^3}, , \qquad (2)$$

where μ – the Earth's gravitational parameter.

Non-centrality of the Earth's gravitational field due to the second zonal harmonic J_2. The main gravitational perturbation considered was the effect of the Earth's nonspherical gravitational field, described by the second zonal harmonic J_2. The corresponding acceleration was calculated using the following formula:

$$a_{J_2} = \frac{3}{2} J_2 \mu \frac{R_\oplus^2}{r^5} \begin{bmatrix} x\left(5\frac{z^2}{r^2} - 1\right) \\ y\left(5\frac{z^2}{r^2} - 1\right) \\ z\left(5\frac{z^2}{r^2} - 3\right) \end{bmatrix} , \qquad (3)$$

where $R_\oplus$ – the Earth's equatorial radius, x,y,z – the coordinates of the spacecraft radius vector.

Scientific Journal of Astana IT University
ISSN (P): 2707-9031 ISSN (E): 2707-904X
VOLUME 25, MARCH 2026

This perturbation causes precession of the ascending node and the argument of perigee, which plays an important role in the formation and maintenance of a sun-synchronous orbit. Atmospheric aerodynamic drag was taken into account by modeling aerodynamic braking as an acceleration:

$$a_{drag} = -\frac{1}{2} C_d \frac{A}{m} \rho(h) \vartheta_{rel}^2 \frac{\mathrm{v}_{rel}}{\|\mathrm{v}_{rel}\|} , \qquad (4)$$

where v_{rel} – the spacecraft velocity relative to the rotating atmosphere.

The atmospheric density $\rho(h)$ was calculated using the empirical NRLMSISE-00 model, which accounts for the spacecraft orbital altitude as well as parameters of solar–geomagnetic activity.

Taking into account the adopted assumptions, the total acceleration acting on the spacecraft was determined by the following expression:

$$\ddot{r} = -\mu \frac{r}{r^3} + a_{J_2} + a_{drag}. \qquad (5)$$

This set of perturbations makes it possible to correctly describe the long-term evolution of the spacecraft orbital elements in low Earth sun-synchronous orbits and adequately reproduces the observed variations of the semi-major axis, eccentricity, and orbital inclination.

In this article, a first-level perturbed motion model is presented, intended for the analysis of long-term orbital evolution and passive deorbiting processes. Figure 1 shows the results of numerical modeling of the long-term evolution of the main orbital elements of the KazEOSat-2 spacecraft in a low Earth sun-synchronous orbit. In particular, the time histories of the semi-major axis (a), eccentricity (e), and orbital inclination (i), expressed in days, are presented.

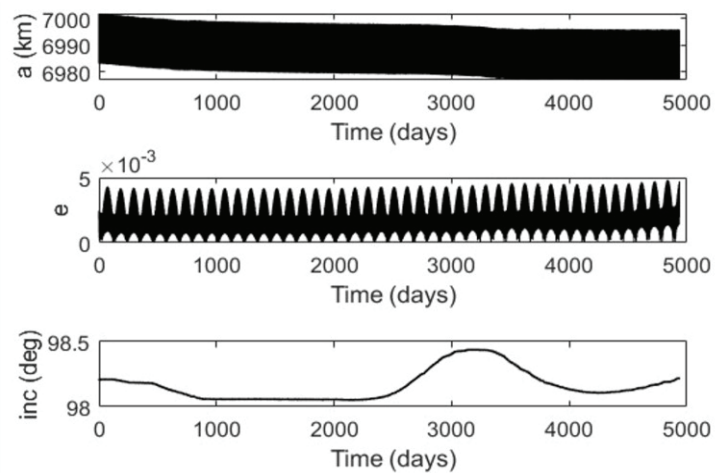

Figure 1. Evolution of the main orbital elements of a spacecraft in a low Earth sun-synchronous orbit

The calculations were performed taking into account the perturbed motion of the spacecraft in a force field that includes the non-centrality of the Earth's gravitational field and atmospheric aerodynamic drag. To model the gravitational field, a model including the second zonal harmonic J_2 was used, which determines the precession of the ascending node and the argument of perigee and ensures the maintenance of the sun-synchronous orbit regime. In addition, long-period perturbations caused by non-axisymmetry of the Earth's gravitational field were included in the model.

Aerodynamic drag was modeled using the empirical NRLMSISE-00 upper atmosphere density model, which accounts for the dependence of density on altitude, geographic location, solar activity level, and geomagnetic conditions. The aerodynamic drag coefficient and the effective aerodynamic cross-sectional area

DOI: 10.37943/25KZEM7835

of the spacecraft were specified as averaged or variable parameters, in accordance with the adopted computational scheme.

The evolution of the semi-major axis $a(t)$ shows a slow, monotonic decrease in its mean value, which is caused by the loss of orbital energy due to aerodynamic drag in the upper atmosphere. Superimposed oscillations reflect the influence of periodic variations in atmospheric density along the orbit and changes in the geometry of motion relative to the incoming flow.

The evolution of the eccentricity $e(t)$ is characterized by quasi-periodic oscillations with an amplitude on the order of 10^{-3}, which corresponds to an almost circular orbit. These oscillations arise as a result of the combined action of the non-central gravitational field of the Earth and aerodynamic perturbations, as well as their periodic modulation along the orbit.

The variation of the orbital inclination $i(t)$ has a smooth, long-period character and is mainly determined by the precessional effect of the second zonal harmonic of the Earth's gravitational field. The observed inclination dynamics correspond to the conditions of a sun-synchronous orbit and confirm that the main gravitational perturbations are correctly accounted for in the model.

Overall, the obtained results confirm that, over the considered time interval, the orbital evolution of the spacecraft is governed by a combination of gravitational perturbations and aerodynamic drag, with aerodynamic drag playing the dominant role in the process of gradual orbital decay. The applied atmospheric model and the adopted perturbation set provide a physically consistent description of long-term orbital dynamics and can be used for further prediction of orbital decay processes and analysis of end-of-life scenarios for spacecraft.

Numerical calculations of the temporal variation of the spacecraft orbital altitude were also performed. The modeling took into account the main gravitational and non-gravitational perturbations. The obtained results demonstrate a combination of short-term orbital oscillations and a long-term decreasing trend in altitude caused by aerodynamic drag in the upper atmosphere. Figure 1 shows the dependence of the spacecraft orbital altitude on time.

The plot exhibits pronounced quasi-periodic oscillations of orbital altitude with an amplitude on the order of several tens of kilometers, superimposed on a slowly decreasing trend of the mean altitude value. These oscillations are explained by the ellipticity of the orbit and reflect the periodic passage of the spacecraft through perigee and apogee. The high frequency of the oscillations corresponds to the orbital period of the spacecraft.

The slow decrease in the mean orbital altitude indicates aerodynamic drag in the upper layers of the atmosphere, which leads to a gradual loss of orbital energy. As the spacecraft descends, it enters denser atmospheric layers, which enhances aerodynamic resistance and accelerates the orbital decay process.

Changes in the amplitude of altitude oscillations over time reflect the evolution of orbital eccentricity and the influence of perturbing factors such as the non-centrality of the Earth's gravitational field and variations in atmospheric density. Despite significant altitude oscillations, the overall trend of the altitude–time dependence $h(t)$ steadily decreases, which corresponds to a scenario of gradual spacecraft deorbiting.

Due to uncertainties in the aerodynamic and configuration parameters of the spacecraft, a single-factor sensitivity analysis of the deorbiting time was performed.

To assess the influence of variations in aerodynamic characteristics, changes in the effective cross-sectional area, aerodynamic drag coefficient, and ballistic coefficient within ranges of ±10% and ±20% relative to the baseline values were considered. The results of this analysis are presented in Table 6.

The following values were adopted as reference (baseline) values for normalization:

m=820 kg

A_0=12.5 m²

C_{d0}=2.2

$B_0=m/(C_{d0}A_0)$=32.73 kg/m²

t_0 – deorbiting time at the baseline values

Scientific Journal of Astana IT University
ISSN (P): 2707-9031 ISSN (E): 2707-904X
VOLUME 25, MARCH 2026

Table 6. Single-factor sensitivity (±10% and ±20%)

Varied parameter	Deviation	Parameter value	New B, kg/m²	Time ratio t/t_0
A	−20%	10.00 m²	40.91	1.25
A	−10%	11.25 m²	36.36	1.11
A	0%	12.50 m²	32.73	1.00
A	+10%	13.75 m²	29.75	0.91
A	+20%	15.00 m²	27.27	0.83
C_d	−20%	1.76	40.91	1.25
C_d	−10%	1.98	36.36	1.11
C_d	0%	2.20	32.73	1.00
C_d	+10%	2.42	29.75	0.91
C_d	+20%	2.64	27.27	0.83
B	−20%	26.18 kg/m²	26.18	0.80
B	−10%	29.45 kg/m²	29.45	0.90
B	0%	32.73 kg/m²	32.73	1.00
B	+10%	36.00 kg/m²	36.00	1.10
B	+20%	39.27 kg/m²	39.27	1.20

As follows from the data in Table 6, an increase in the effective aerodynamic cross-sectional area of the spacecraft by 20% reduces the calculated deorbiting time by approximately 15–20% relative to the baseline case. A similar effect is observed when the aerodynamic drag coefficient is increased, which is equivalent to a decrease in the ballistic coefficient.

At the same time, an increase in the ballistic coefficient by 20% leads to an approximately 20% increase in the calculated orbital decay time. These dependencies confirm the dominant role of the ballistic coefficient in the rate of passive deorbiting and demonstrate the high sensitivity of the results to the aerodynamic and structural parameters of the spacecraft.

Thus, the presented plot clearly illustrates the combination of rapid orbital oscillations and a slow decrease in orbital altitude that governs the deorbiting process of a spacecraft in the absence of active control.

From the $h(t)$ curve, the rate of decrease in the mean orbital altitude can be estimated as difference between the average altitude levels at the beginning and the end of the simulation interval divided by duration of this interval. For the KazEOSat-2 spacecraft, over the considered time span from $t = 0$ to $t \approx 5000$ days (≈13.7 years), the mean altitude level decreases approximately from 617–618 km to 610–611 km. Consequently, the total decrease in the mean altitude is about $\Delta h \approx 7$ km over ~13.7 years, which yields the following estimate of the average orbital decay rate:

$$\overline{\frac{dh}{dt}} \approx \frac{\Delta \bar{h}}{\Delta t} \approx \frac{7\ km}{13{,}7\ year} \approx 0{,}5\ km/year. \qquad (6)$$

Taking into account the limited accuracy of reading data from the plot and the fluctuations in atmospheric density, for this computational scenario, it is reasonable to report a range for the mean annual decrease in altitude: 0.4–0.7 km/year.

Atmospheric density modeling. Figure 2 presents the results of calculating the upper-atmosphere density ρ_{air} during the spacecraft orbital motion. The upper plot shows the time evolution of density, while the lower plot shows its dependence on the current orbital altitude h.

The $\rho_{\text{air}}(t)$ curve demonstrates pronounced non-stationarity of atmospheric density throughout the entire modeling period. High-frequency oscillations are caused by diurnal and orbital variations associated with changes in the spacecraft's geographic position, local solar illumination, and its relative velocity through

DOI: 10.37943/25KZEM7835

the atmosphere. Long-period variations reflect the influence of solar and geomagnetic activity, including phases of the solar cycle, which leads to a noticeable increase in mean density during certain periods.

The change in the oscillation pattern of density near the end of the time interval is associated with orbital decay and the spacecraft's transition into denser layers of the upper atmosphere. In this region, the contribution of aerodynamic drag increases significantly, which enhances density oscillations and, consequently, intensifies orbital braking.

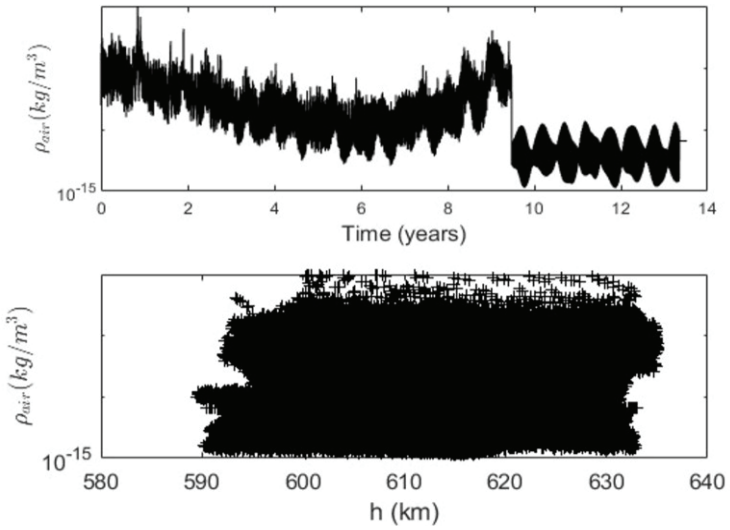

Figure 2. Atmospheric density

The $\rho_{\text{air}}(h)$ plot shows the dependence of atmospheric density on altitude for orbits in the range of 580–640 km, which is typical for KazEOSat-2. The scatter of points in the plot indicates that atmospheric density at a given altitude is not a single-valued function of height, but depends on time, the level of solar activity, and geomagnetic conditions. Even small changes in orbital altitude can lead to variations in atmospheric density by an order of magnitude or more, which is a characteristic feature of the Earth's upper atmosphere.

Overall, the plots demonstrate the high variability of atmospheric density in low Earth orbits and its significant impact on the spacecraft deorbiting process. The obtained results confirm the necessity of using empirical atmospheric models that account for solar–geomagnetic parameters, as well as performing parametric and scenario-based calculations when forecasting orbital decay and end-of-life timelines for spacecraft.

Aerodynamic drag. The time dependence of the aerodynamic drag power (P_{drag}) acting on the spacecraft in orbit is shown in Figure 3. The horizontal axis represents the simulation time in days, while the vertical axis shows the aerodynamic drag power in watts.

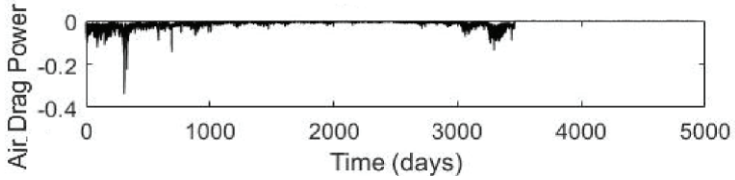

Figure 3. Aerodynamic drag power of the spacecraft

The negative power over the considered simulation interval indicates the dissipative nature of aerodynamic drag, which causes an irreversible loss of the mechanical energy of the spacecraft's orbital motion. The aerodynamic drag power, determined by the work of the atmospheric drag force, can be expressed as follows:

Scientific Journal of Astana IT University
ISSN (P): 2707-9031 ISSN (E): 2707-904X
VOLUME 25, MARCH 2026

$$P_{drag}=F_{drag}.v \ , \qquad (7)$$

where F_{drag} is the aerodynamic drag force and v is the spacecraft velocity relative to the atmosphere.

High-frequency oscillations of the power are caused by several factors: variations in upper-atmosphere density along the orbit, changes in relative velocity and spacecraft attitude, as well as diurnal and orbital effects. Individual sharp drops in power correspond to passages through orbital regions with increased atmospheric density, which may be caused both by geographic inhomogeneity of the atmosphere and by periods of enhanced solar–geomagnetic activity.

Despite the fact that the absolute magnitude of aerodynamic drag power is small, which is typical for low Earth orbits (630–750 km) occupied by the Kazakh Earth remote sensing spacecraft, its prolonged action over long-time intervals leads to a noticeable reduction in orbital energy. This, in turn, results in a gradual decrease of the orbital semi-major axis, which is confirmed by the simulation results of orbital element evolution.

Thus, the plot demonstrates the cumulative effect of aerodynamic drag and its important role in the process of long-term passive deorbiting of spacecraft, even at small instantaneous power levels.

The negative aerodynamic drag power $P_{drag}(t)$ is directly related to the decrease in orbital energy and, consequently, to the gradual reduction of the orbital semi-major axis $a(t)$. For a Keplerian orbit, the specific mechanical energy of the spacecraft motion is expressed as:

$$\varepsilon = -\frac{\mu}{2a} \ , \qquad (8)$$

where μ is the Earth's gravitational parameter. Since aerodynamic drag performs negative work, the rate of change of energy is related to the drag power as:

$$\frac{d\varepsilon}{dt} = \frac{1}{m} P_{drag}(t) \ . \qquad (9)$$

Differentiation of the expression for ε makes it possible to establish a relationship between the change in the semi-major axis and the aerodynamic drag power:

$$\frac{d\varepsilon}{dt} = \frac{\mu}{2a^2}\frac{da}{dt}, \qquad => \frac{da}{dt} = \frac{2a^2}{\mu m} P_{drag}(t) \ . \qquad (10)$$

From the $P_{drag}(t)$ curve, it is evident that $P_{drag}(t) < 0$ (Figure 3). Consequently, from the last expression it follows that $da/dt < 0$, i.e., the orbital semi-major axis decreases. Negative peaks in the $P_{drag}(t)$ plot, corresponding to more intense aerodynamic drag, are characterized by a short-term increase in the magnitude of da/dt. This leads to a more rapid decrease of $a(t)$ over the corresponding time intervals.

Thus, the aerodynamic drag power plot can be regarded as an energetic interpretation of the deorbiting process: the prolonged action of negative power results in a cumulative loss of orbital energy and, consequently, in a steady decrease of the orbital semi-major axis over time.

Discussion

The results of the study demonstrate a substantial difference in the passive orbital decay time between KazEOSat-1 and KazEOSat-2. The factors governing this difference are the spacecraft's ballistic coefficient and the atmospheric density at the corresponding orbital altitude.

For a comparative assessment of these differences, an approximate calculation of the ratio of orbital decay times was performed (Table 7). The calculations show that the higher ballistic coefficient and significantly greater orbital altitude of KazEOSat-1 lead to markedly weaker aerodynamic drag compared to KazEOSat-2. Consequently, the predicted passive deorbiting time of KazEOSat-1 exceeds that of KazEOSat-2 by an order of magnitude or more.

DOI: 10.37943/25KZEM7835

Table 7. Estimated ratio of orbital decay times for KazEOSat-1 and KazEOSat-2

Evaluation component	**Notation**	**Range (based on previously adopted estimates)**	**Comment**
Ratio of ballistic coefficients	B_{k1}/ B_{k2}	1.5 – 5.6	For B_{k1}≈25–45 kg/m² and B_{k2}≈8–17 kg/m²
Ratio of atmospheric densities at orbital altitudes	ρ(630)/ρ(750)	5 – 30	Strongly depends on solar activity and the atmospheric model; at 630 km the density is noticeably higher than at 750 km.
Overall estimated ratio of decay times	t_{k1}/t_{k2}	7 – 170	Obtained as the product of the two factors above.

In addition to the indicative range presented above, a more representative estimate can be obtained from the baseline numerical simulation under a consistent set of aerodynamic parameters. Based on the adopted reference values, the ratio of passive deorbiting times for KazEOSat-1 and KazEOSat-2 is estimated to be on the order of 10–30. This value reflects the expected difference in orbital lifetime under typical conditions and provides a more practical reference point, while the wider range given in Table 7 accounts for uncertainties in atmospheric density and aerodynamic characteristics.

The presented estimate is indicative, but it is consistent with the results of numerical modeling, which indicate slow orbital evolution of KazEOSat-1 and a more rapid orbital decay of KazEOSat-2. The likelihood of meeting the international recommendation of deorbiting within 25 years for both spacecraft without the use of active deorbiting systems appears to be low.

It should be emphasized that the given estimate of the ratio of orbital decay times is of an indicative nature and reflects a range of possible passive deorbiting scenarios rather than a fixed deterministic value. This spread is due to the high variability of upper-atmosphere density, which at the considered altitudes strongly depends on the level of solar–geomagnetic activity and the selected atmospheric model. In practice, this means that even with unchanged ballistic characteristics of a spacecraft, the actual rate of aerodynamic drag may differ significantly from average calculated estimates.

The obtained results allow a practical conclusion to be drawn regarding the significant limitations of passive deorbiting for spacecraft operating in sun-synchronous orbits at altitudes of about 750–760 km. For the KazEOSat-1 satellite, operating within this altitude range, atmospheric density remains extremely low; therefore, even under favorable solar activity conditions, aerodynamic drag is insufficient to ensure effective deorbiting within reasonable timeframes.

For the KazEOSat-2 satellite, operating in a lower sun-synchronous orbit, passive deorbiting represents a more realistic scenario; however, the deorbiting timelines in this case remain sensitive to the aerodynamic configuration and ballistic parameters of the spacecraft, which limits the universality of this approach.

Conclusion

The conducted study made it possible to quantitatively and qualitatively assess the features of passive deorbiting of the Kazakh Earth remote sensing spacecraft KazEOSat-1 and KazEOSat-2. Numerical modeling of orbital dynamics revealed significant differences in the rates of passive orbital decay of these spacecrafts. For KazEOSat-2, the average rate of orbital altitude decrease is 0.4–0.7 km per year, whereas for KazEOSat-1 it is significantly lower and characterized by greater inertia. This deviation from generalized estimates for typical sun-synchronous orbits is primarily explained by the lower orbital altitude and associated increase in aerodynamic drag.

Scientific Journal of Astana IT University
ISSN (P): 2707-9031 ISSN (E): 2707-904X
VOLUME 25, MARCH 2026

The sensitivity analysis showed that variations in the effective aerodynamic cross-sectional area and the aerodynamic drag coefficient within ±20% lead to changes in the calculated deorbiting time by 15–25%. In contrast to studies where aerodynamic parameters are fixed, this result highlights the importance of accounting for uncertainties in spacecraft configuration, since these parameters directly affect the ballistic coefficient and, consequently, the rate of orbital energy loss.

A comparative assessment of passive deorbiting timelines showed that the ratio of orbital decay times for KazEOSat-1 to KazEOSat-2 can vary from 10 to 100 or more, depending on scenarios of aerodynamic parameter variations and the level of solar activity. The substantial divergence in deorbiting times compared to previously published generalized estimates is explained by the combined effect of the higher orbital altitude of KazEOSat-1 and the significantly lower atmospheric density at these altitudes, given comparable values of the aerodynamic drag coefficient.

Acknowledgment

The study was carried out with the financial support of the Science Committee of the Ministry of Science and Higher Education of the Republic of Kazakhstan for 2025–2027 (Grant No. AP26103099).

References

[1] Zhumazhanov, B., Kulakayeva, A., Ashurov, A., Baktybekov, K., Zhetpisbayeva, A., Uskenbaev, D., Zhumazhanov, B., Zylgara, A., & Kargulova, A. (2024). Devising a deorbitation strategy for Kazakhstani's KazEOSat-1 spacecraft. *Eastern-European Journal of Enterprise Technologies*, *6*(5 (132), 49–62. https://doi.org/10.15587/1729-4061.2024.319226

[2] Mahapatra, Sukdev. (2025). Modeling Orbital Decay of Low-Earth Orbit Satellites due to Atmospheric Drag: A Simplified Analytical Approach. https://doi.org/10.48550/arXiv.2508.19549.

[3] Rosengren, A. J., Skoulidou, D. K., Tsiganis, K., & Voyatzis, G. (2019). Dynamical cartography of Earth satellite orbits. *Advances in Space Research, 63*(1), 443–460. https://doi.org/10.1016/j.asr.2018.09.004

[4] Smith, B. G. A., Capon, C. J., Brown, M., & Boyce, R. R. (2020). Ionospheric drag for accelerated deorbit from upper low Earth orbit. *Acta Astronautica, 176*, 520–530. https://doi.org/10.1016/j.actaastro.2020.07.007

[5] Sánchez-Arriaga, G., Sanmartín, J. R., & Lorenzini, E. C. (2017). Comparison of technologies for deorbiting spacecraft from low-Earth orbit at end of mission. *Acta Astronautica, 138*, 536–542. https://doi.org/10.1016/j.actaastro.2016.12.004

[6] Palla, C., & Kingston, J. (2016). Forecast analysis on satellites that need de-orbit technologies: Future scenarios for passive de-orbit devices. *CEAS Space Journal, 8*(3), 191–200. https://doi.org/10.1007/s12567-016-0120-x

[7] Jackson, D. R., Bruinsma, S., Negrin, S., Stolle, C., Budd, C. J., Gonzalez, R. D., & Zhelavskaya, I. S. (2020). The space weather atmosphere models and indices (SWAMI) project: Overview and first results. *Journal of Space Weather and Space Climate, 10*, 18. https://doi.org/10.1051/swsc/2020019

[8] Vielberg, K., Forootan, E., Lück, C., Löcher, A., Kusche, J., & Börger, K. (2018). Comparison of accelerometer data calibration methods used in thermospheric neutral density estimation. *Annales Geophysicae, 36*(3), 761–779. https://doi.org/10.5194/angeo-36-761-2018

[9] Niccolai, L., & Mengali, G. (2024). Decay time estimate for LEO spacecraft. *Acta Astronautica*, *225*, 601-614. https://doi.org/10.1016/j.actaastro.2024.09.045

[10] Walsh, J., Berthoud, L., & Allen, C. (2021). Drag reduction through shape optimisation for satellites in very low Earth orbit. *Acta Astronautica, 179*, 105–121. https://doi.org/10.1016/j.actaastro.2020.09.018

[11] Alshamy, H. M., Makled, A. E. S., Elhalwagy, Y., & Hendy, H. (2019). Flight dynamic model for low Earth orbit satellites. In *Proceedings of the 18th International Conference on Aerospace Sciences and Aviation Technology* (pp. 1–12). Military Technical College. https://doi.org/10.1088/1757-899X/610/1/012100

[12] Official website of JSC «NC «Qazaqstan Gharysh Sapary»». (n.d.). Retrieved December 9, 2025, from https://www.gharysh.kz/

[13] Minister of Digital Development, Innovations, and Aerospace Industry of the Republic of Kazakhstan. (2025) *Order No. 645/NQ dated December 12, 2025* [in Russian].

DOI: 10.37943/25KZEM7835

[14] Innoter. (n.d.). *Satellites* [in Russian]. Retrieved December 9, 2025, from https://innoter.com/sputniki/

[15] Inform.kz. (2017, April 30). *Kazakh satellite KazEOSat-1 captured 370 thousand images from space* [in Russian]. Retrieved December 12, 2025, from https://www.inform.kz/ru/kazahstanskiy-sputnik-kazeosat-1-otsnyal-370-tysyach-snimkov-iz-kosmosa_a3022221

[16] N2YO.com. (n.d.). *KAZEOSAT-1 satellite details (NORAD ID 39731)*. Retrieved December 12, 2025, from https://www.n2yo.com/satellite/?s=39731

[17] Gunter's Space Page. (n.d.). *KazEOSat-1 / KazEOSat-2*. Retrieved December 12, 2025, from https://space.skyrocket.de/doc_sdat/kazeosat-1.htm

[18] eoPortal. (n.d.). *KazEOSat-1*. Retrieved December 12, 2025, from https://www.eoportal.org/satellite-missions/kazeosat-1

[19] Sánchez-Arriaga, G., Borderes-Motta, G., & Chiabó, L. (2022). A code for the analysis of missions with electrodynamic tethers. *Acta Astronautica, 198*, 51–62. https://doi.org/10.1016/j.actaastro.2022.06.021

[20] García Ortiz, J. J., & Sánchez-Arriaga, G. (2025). A severing rate model for tape tethers based on experimental ballistic equations. *Advances in Space Research*. https://doi.org/10.1016/j.asr.2025.03.014